

FREE-SURFACE DYNAMICS OF THIN SECOND-GRADE FLUID OVER AN UNSTEADY STRETCHING SHEET

S. PANDA^{✉1}, K. K. PATRA¹ and M. SELLIER²

(Received 10 May, 2017; accepted 22 June, 2018; first published online 5 November 2018)

Abstract

We derive an evolution equation for the free-surface dynamics of a thin film of a second-grade fluid over an unsteady stretching sheet using long-wave theory. For the numerical investigation of the viscoelastic effect on the thin-film dynamics, a finite-volume approach on a uniform grid with implicit flux discretization is applied. The present results are in excellent agreement with results available in the literature for a Newtonian fluid. We observe that the fluid thins faster with the rapid stretching rate of the sheet, but the second-grade parameter delays the thinning behaviour of the liquid film.

2010 *Mathematics subject classification*: primary 76A20; secondary 76A05.

Keywords and phrases: thin liquid film, stretching sheet, second-grade fluid, free-surface flow, long-wave theory, finite-volume method.

1. Introduction

In the context of metal and polymer extrusion, continuous casting, drawing of plastic sheets, or cable coating, a model reduction of the two-phase Navier–Stokes equations based on the plane-interface assumption is a well-known technique and it is still a subject of research. The uniform film thickness assumption in the domain enables a similarity transformation which reduces the set of partial differential equations to a set of ordinary differential equations (ODEs). The resulting ODEs are relatively easy to solve either analytically or numerically. Crane [5] first gave an exact similarity solution in closed analytic form and numerically solved the steady, two-dimensional, boundary layer flow problem due to the linear variation of a flat stretching sheet. A reduced ODE model was developed by Wang [26] for an unsteady thin fluid film lying on an accelerating stretching surface. Later, Andersson et al. [3] and Liu and Andersson [17]

¹Department of Mathematics, National Institute of Technology Calicut, NIT (P.O.)-673601, Kerala, India; e-mail: satyanand@nitc.ac.in, kirankumar_p140033ma@nitc.ac.in.

²Department of Mechanical Engineering, The University of Canterbury, Private Bag 4800, Christchurch 8140, New Zealand; e-mail: mathieu.sellier@canterbury.ac.nz.

© Australian Mathematical Society 2018

extended Wang's contribution by analysing the associated heat transfer problem. Noor et al. [19] derived a similar set of ODEs for the nonisothermal magnetohydrodynamics (MHD) flow of a thin liquid film over an unsteady elastic stretching surface. The derivation of the self-similar equations for the description of the MHD power-law fluid over a stretching sheet was given by Andersson et al. [4]. Many recent studies have focused on the derivation of self-similar boundary layer equations for the unsteady thin-film flow of a Newtonian [9] and a non-Newtonian fluid [2]. For example, the analysis for the derivation of the self-similar model for the second-grade fluid flow over an unsteady stretching sheet was explained by Abbas et al. [1]. The discussion was later extended for the derivation of a simplified system of ODEs in the boundary layer assumption framework in the context of thin-film flow of second-grade fluid with temperature-dependent viscosity [18].

Thus, many of the aforementioned research works are devoted to the development of models for the study of thin-film flow over a stretching sheet in the boundary layer approximation framework. The construction of a one-dimensional thin-film equation of a Newtonian fluid over a stretching sheet with the assumption that the liquid mass is completely covered by the boundary layer was first studied by Dandapat et al. [6, 7] for uniform thickness and later by the same authors [8] for the nonplanar film thickness at the onset of stretching.

Our work focuses on the systematic derivation of the thin-film equation for a second-grade non-Newtonian fluid over an unsteady stretching sheet, analogous to that of Santra et al. [24] without the restriction of the plane-interface assumption. One motivation for this study is the flow of mucus in biological tissues which undergo expansion or contraction. A particular example is pulmonary alveoli which are covered with a lining of non-Newtonian fluid [16] and which undergo periodic expansion and contraction.

The paper is organized as follows. In the next section, the governing equations for the flow of second-grade fluid over an unsteady stretching sheet are described. In Section 3, the long-wave approximation for the derivation of the thin-film equation is presented. The numerical procedure for the solution of the derived equation is explained in Section 4. In Section 5, we discuss the numerical results and, finally, Section 6 is devoted to conclusions.

2. Formulation of the problem

We study an unsteady flow of an incompressible, non-Newtonian second-grade liquid film on a flat elastic sheet as shown in Figure 1. The flow over the elastic sheet is along the x -direction and the normal to the plane is taken as the z -axis. We assume that initially the surface of the sheet is at rest having an initial thickness h_0 , starts stretching from rest suddenly at $t = 0^+$, and acquires the nonlinear stretching velocity $U(x, t)$. The gravitational acceleration g is acting vertically downward along the negative z -direction. We assume that the liquid is nonvolatile and so thin that we can ignore the effects of evaporation and buoyancy.

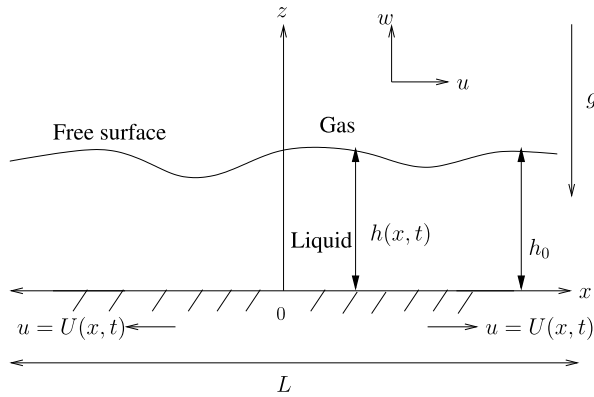


FIGURE 1. Sketch of flow geometry.

The motion of the second-grade fluid due to the stretching sheet is governed by the continuity equation of mass flow and the momentum equation:

- continuity equation

$$\nabla \cdot \mathbf{V} = 0, \tag{2.1}$$

- momentum equation

$$\rho \frac{D\mathbf{V}}{Dt} = \nabla \cdot \boldsymbol{\tau} + \rho \mathbf{g}, \tag{2.2}$$

where $\mathbf{V}(x, z, t) = (u(x, z, t), w(x, z, t))$ is the velocity vector at position (x, z) and time t . The symbol ρ stands for the density of the fluid and $\boldsymbol{\tau}$ is the Cauchy stress tensor.

The boundary conditions on the stretching sheet at $z = 0$ are due to no slip and no penetration on the surface and are given by

$$u(x, 0, t) = U(x, t) \quad \text{and} \quad w(x, 0, t) = 0. \tag{2.3}$$

At the free surface $z = h(x, t)$, the boundary conditions are due to the balance of stresses and the kinematic condition:

$$p_a + \hat{\mathbf{n}} \cdot \boldsymbol{\tau} \cdot \hat{\mathbf{n}} = -\sigma(\nabla \cdot \hat{\mathbf{n}}), \tag{2.4}$$

$$\hat{\mathbf{n}} \cdot \boldsymbol{\tau} \cdot \hat{\mathbf{t}} = 0 \tag{2.5}$$

and

$$h_t + uh_x = w, \tag{2.6}$$

where $\hat{\mathbf{n}}$ and $\hat{\mathbf{t}}$ are the unit normal and tangential vectors on the surface, respectively. Here p_a is the atmospheric pressure at the free surface and σ stands for the constant surface tension of the fluid. The subscripts x and t stand for the partial differential equation with respect to x and t , respectively.

Following Kalliadasis et al. [15], the kinematic boundary condition equation (2.6) is obtained by differentiating $z - h(x, t) = 0$ with respect to t , that is, $(D/Dt)(z - h) = 0$.

The initial conditions are

$$u(x, z, 0) = w(x, z, 0) = 0 \quad \text{and} \quad h(x, 0) = h_0 + \delta(x), \tag{2.7}$$

where h_0 is the characteristic height of the free surface and $\delta(x)$ is the small disturbance to h_0 .

The *Cauchy stress tensor*, given by Rivlin and Ericksen [23] for a second-grade fluid, can be written as

$$\boldsymbol{\tau} = -p\mathbf{I} + \mu\mathbf{A}_1 + \alpha_1\mathbf{A}_2 + \alpha_2\mathbf{A}_1^2, \tag{2.8}$$

where p is the pressure, \mathbf{I} is the identity tensor, and μ is the coefficient of viscosity. Here the material constants α_1 and α_2 are the first and second normal stress coefficients. The quantities \mathbf{A}_i ($i = 1, 2$) are the Rivlin–Ericksen tensors, which are defined recursively as

$$\mathbf{A}_0 = \mathbf{I}, \tag{2.9a}$$

$$\mathbf{A}_i = \frac{D}{Dt}\mathbf{A}_{i-1} + \mathbf{A}_{i-1} \cdot (\nabla\mathbf{V}) + (\nabla\mathbf{V})^* \cdot \mathbf{A}_{i-1}, \tag{2.9b}$$

where D/Dt is the material time derivative and the superscript $(*)$ is used for the transpose of the matrix $\nabla\mathbf{V}$.

The constitutive model equation (2.8) is derived by considering a second-order approximation of the retardation parameter. Dunn and Fosdick [10] have shown that this model equation is invariant under transformation and, therefore, the material constants must meet the restriction

$$\mu \geq 0, \quad \alpha_1 \geq 0, \quad \alpha_1 + \alpha_2 = 0. \tag{2.10}$$

Fluids characterized by these restrictions in equation (2.10) are called second-grade fluids. The fluid model represented by equation (2.8) with the relationship (2.10) is compatible with the hydrodynamics. The third relation in equation (2.10) is the consequence of satisfying the Clausis–Duhem inequality [22] by fluid motion and a second relation arises due to the assumption that the specific Helmholtz free energy of the fluid takes its minimum value in equilibrium. Generally, a fluid satisfying the model equation (2.8) with $\alpha_i < 0$ ($i = 1, 2$) is named a second-order fluid and, with $\alpha_i > 0$, is named a second-grade fluid. Although a second-order fluid obeying model equation (2.8) with $\alpha_1 < \alpha_2$, $\alpha_1 < 0$, exhibits unstable solutions [12], the second-order approximation is valid at low shear rate [11].

We next scale the film thickness with the characteristic height of the flow $h = h_0\tilde{h}$ and $\delta(x) = h_0\tilde{\delta}(x)$, the coordinates by the characteristic length of the domain $(x, z) = L(\tilde{x}, \tilde{z})$, and the velocity $(u, w) = (\nu\tilde{u}/h_0, \epsilon\nu\tilde{w}/h_0)$, $U = (\nu/h_0)\tilde{U}$, the time $t = (h_0^2/\epsilon\nu)\tilde{t}$, and the pressure $p = p_a + (\rho\nu^2/\epsilon h_0^2)\tilde{p}$. Here $\epsilon = h_0/L$ is the aspect ratio and $\nu = \mu/\rho$ is the kinematic viscosity of the fluid. Using the constitutive relation equation (2.8) with equations (2.9a) and (2.9b) and the constraint equation (2.10), the nondimensional form of the governing equations (2.1)–(2.2), after dropping the tilde symbol, in explicit form are

$$u_x + w_z = 0, \tag{2.11}$$

$$\begin{aligned} \epsilon(u_t + uu_x + wu_z) = & -p_x + \epsilon^2 u_{xx} + u_{zz} + K(\epsilon^3 u_{xxt} + \epsilon u_{zzt} + \epsilon^3 uu_{xxx} - \epsilon uw_{zzz} \\ & + \epsilon^3 u_x u_{xx} - \epsilon u_x u_{zz} + \epsilon^3 wu_{xz} + \epsilon wu_{zzz} - 4\epsilon^3 w_x w_{zz} \\ & - 2\epsilon^5 w_x w_{xx} + \epsilon^3 u_z w_{xx} - \epsilon u_z w_{zz} + 2\epsilon w_z u_{zz}) \end{aligned} \quad (2.12)$$

and

$$\begin{aligned} \epsilon^3(w_t + uw_x + ww_z) = & -p_z + \epsilon^4 w_{xx} + \epsilon^2 w_{zz} + K(\epsilon^4 w_{xxt} + \epsilon^2 w_{zzt} + \epsilon^2 uw_{zzz} + \epsilon^4 uw_{xxx} \\ & + 2\epsilon^4 u_x w_{xx} + \epsilon^2 w_x u_{zz} - \epsilon^4 w_x u_{xx} + \epsilon^2 ww_{zzz} - \epsilon^4 wu_{xxx} \\ & + \epsilon^2 w_z w_{zz} - \epsilon^4 w_z w_{xx} - 4\epsilon^2 u_z u_{xx} - 2u_z u_{zz}) - \epsilon \text{Fr}. \end{aligned} \quad (2.13)$$

The dimensional numbers are the viscoelastic parameter $K = \alpha_1/\rho h_0^2$, which relates to the first- and second-order normal stress coefficients, and the modified Froude number $\text{Fr} = gh_0^3/\nu^2$.

The boundary condition equations (2.3)–(2.6) can be written in nondimensional form

$$\text{at } z = 0, \quad u(x, 0, t) = U(x, t), \quad w(x, 0, t) = 0. \quad (2.14)$$

At the free surface $z = h(x, t)$,

$$\begin{aligned} & -(\epsilon^2 h_x^2 + 1)p + 2\epsilon^2(\epsilon^2 h_x^2 u_x - \epsilon^2 h_x w_x - h_x u_z + w_z) + K\epsilon^3(2\epsilon^2 u_{tx} h_x^2 - 2\epsilon^2 h_x w_{tx} \\ & - 2h_x u_{tz} + 2w_{tz}) + K\epsilon[\epsilon^2 h_x^2(2\epsilon^2 uu_{xx} + 2\epsilon^2 wu_{xz} + u_z^2 - \epsilon^4 w_x^2) - 2\epsilon^2 h_x \\ & \times (\epsilon^2 uw_{xx} + uu_{xz} + \epsilon^2 ww_{xz} + wu_{zz} + \epsilon^2 u_x w_x - \epsilon^2 w_x w_z + u_z w_z - u_x u_z) \\ & + 2\epsilon^2 uw_{xz} + 2\epsilon^2 ww_{zz} + \epsilon^4 w_x^2 - u_z^2] \\ & = \epsilon S h_{xx}(\epsilon^2 h_x^2 + 1)^{-1/2}, \end{aligned} \quad (2.15)$$

$$\begin{aligned} & (\epsilon^2 w_x + u_z)(1 - \epsilon^2 h_x^2) + 2\epsilon^2 h_x(w_z - u_x) \\ & + K[(1 - \epsilon^2 h_x^2)(\epsilon^3 w_{tx} + \epsilon u_{tz}) + 2\epsilon^3 h_x(w_{tz} - u_{tx})] \\ & + K[(1 - \epsilon^2 h_x^2)(\epsilon^3 uw_{xx} + \epsilon uu_{xz} + \epsilon^3 ww_{xz} + \epsilon wu_{zz} + \epsilon^3 u_x w_x - \epsilon^3 w_x w_z + \epsilon u_z w_z \\ & - \epsilon u_x u_z) + 2\epsilon h_x(\epsilon^2 uw_{xz} + \epsilon^2 ww_{zz} - \epsilon^2 uu_{xx} - \epsilon^2 wu_{xz} + \epsilon^4 w_x^2 - u_z^2)] \\ & = 0 \end{aligned} \quad (2.16)$$

and

$$h_t + uh_x = w. \quad (2.17)$$

The symbol S stands for the nondimensional surface tension parameter defined as $S = \epsilon^2 \sigma h_0/\rho\nu^2$. The equations (2.15) and (2.16) are obtained after using the expression for the unit normal vector $\hat{\mathbf{n}} = (-h_x/\sqrt{1+h_x^2}, 1/\sqrt{1+h_x^2})$ and the unit tangent vector $\hat{\mathbf{t}} = (1/\sqrt{1+h_x^2}, h_x/\sqrt{1+h_x^2})$. The initial conditions (2.7) in dimensionless form read as

$$u = 0, \quad w = 0, \quad \text{and} \quad h(x, 0) = 1 + \delta(x).$$

3. Long-wave approximation

The derivation of the one-dimensional thin-film equation is based on long-wave theory. Thereby, the asymptotic expansions in zeroth, first, and second order yield the necessary evolution equation of the film height for the second-grade fluid model. The stated asymptotic analysis uses the techniques of Santra et al. [24], but extends it to incorporate the complex rheological effects. Clearly, the smaller the value of ϵ , the better the approximation, but lubrication theory has been known to produce accurate results even in a parameter range arguably outside its validity window [20].

To obtain the equation of the thin film from the underlying problem, the regular power series expansion in aspect ratio ϵ is set up for the flow variables. Accordingly [24],

$$(u, w, p) = (u_0, w_0, p_0) + \epsilon(u_1, w_1, p_1) + \epsilon^2(u_2, w_2, p_2) + \dots \tag{3.1}$$

As per the scaling, the viscoelastic parameter K and the Froude number Fr are of order $O(1)$, and the surface tension parameter S is of order $O(\epsilon^2)$. Substituting equation (3.1) in the nondimensional equations (2.11)–(2.17) and equating the coefficient of ϵ^n , $n = 0, 1, 2$, we get solutions to problems of the following orders.

3.1. Zeroth order The leading order equations are

$$\frac{\partial u_0}{\partial x} + \frac{\partial w_0}{\partial z} = 0, \tag{3.2}$$

$$-\frac{\partial p_0}{\partial x} + \frac{\partial^2 u_0}{\partial z^2} = 0, \tag{3.3}$$

$$\text{and } \frac{\partial p_0}{\partial z} = 0. \tag{3.4}$$

The boundary conditions are

$$\text{at } z = 0 : u_0 = U(x, t), \quad w_0 = 0, \tag{3.5}$$

$$\text{and at } z = h(x, t) : p_0 = 0, \quad \frac{\partial u_0}{\partial z} = 0. \tag{3.6}$$

Using the stream function $\psi_0 = U(x, t)z$, the solution of the zeroth-order problem (equations (3.2)–(3.6)) is

$$u_0 = U(x, t), \quad w_0 = -z U_x(x, t), \quad \text{and } p_0 = 0. \tag{3.7}$$

3.2. First order The first-order problem reads

$$\frac{\partial u_1}{\partial x} + \frac{\partial w_1}{\partial z} = 0, \tag{3.8}$$

$$\begin{aligned} \frac{\partial u_0}{\partial t} + u_0 \frac{\partial u_0}{\partial x} + w_0 \frac{\partial u_0}{\partial z} = & -\frac{\partial p_1}{\partial x} + \frac{\partial^2 u_1}{\partial z^2} + K \left(\frac{\partial^3 u_0}{\partial t \partial z^2} - u_0 \frac{\partial^3 w_0}{\partial z^3} - \frac{\partial u_0}{\partial x} \frac{\partial^2 u_0}{\partial z^2} \right. \\ & \left. + w_0 \frac{\partial^3 u_0}{\partial z^3} - \frac{\partial u_0}{\partial z} \frac{\partial^2 w_0}{\partial z^2} + 2 \frac{\partial w_0}{\partial z} \frac{\partial^2 u_0}{\partial z^2} \right), \end{aligned} \tag{3.9}$$

and

$$-\frac{\partial p_1}{\partial z} + K\left[-2\frac{\partial u_0}{\partial z}\frac{\partial^2 u_0}{\partial z^2}\right] - Fr = 0. \tag{3.10}$$

The boundary conditions are

$$\text{at } z = 0, u_1 = 0, \quad w_1 = 0, \tag{3.11}$$

and, at the free surface $z = h(x, t)$,

$$-p_1 - K\left(\frac{\partial u_0}{\partial z}\right)^2 = S h_{xx} \tag{3.12}$$

and

$$\frac{\partial u_1}{\partial z} + K\left(\frac{\partial^2 u_0}{\partial t \partial z} + u_0 \frac{\partial^2 u_0}{\partial x \partial z} + w_0 \frac{\partial^2 u_0}{\partial z^2} + \frac{\partial u_0}{\partial z} \frac{\partial w_0}{\partial z} - \frac{\partial u_0}{\partial x} \frac{\partial u_0}{\partial z} - 2h_x \left(\frac{\partial u_0}{\partial z}\right)^2\right) = 0. \tag{3.13}$$

Equations (3.12) and (3.13) are obtained by considering ϵ terms after expansion from equations (2.15) and (2.16).

Using the solution (equation (3.7)) of the zeroth-order problem, the solution of the first-order problem (equations (3.8)–(3.13)) for the velocity and pressure is

$$u_1 = f(x, t)\left(\frac{z^2}{2} - hz\right), \tag{3.14}$$

$$w_1 = -\frac{z^3}{6} f_x(x, t) + \frac{z^2}{2} (hf(x, t))_x, \tag{3.15}$$

$$p_1 = Fr(h - z) - S h_{xx}. \tag{3.16}$$

For brevity, we introduce the notation $f(x, t) = U_t + UU_x + Fr h_x - S h_{xxx}$.

3.3. Second order The equations for the second-order problem are

$$\frac{\partial u_2}{\partial x} + \frac{\partial w_2}{\partial z} = 0, \tag{3.17}$$

$$\begin{aligned} & \frac{\partial u_1}{\partial t} + u_0 \frac{\partial u_1}{\partial x} + u_1 \frac{\partial u_0}{\partial x} + w_0 \frac{\partial u_1}{\partial z} + w_1 \frac{\partial u_0}{\partial z} \\ &= -\frac{\partial p_2}{\partial x} + \frac{\partial^2 u_0}{\partial x^2} + \frac{\partial^2 u_2}{\partial z^2} + K\left(\frac{\partial^3 u_1}{\partial t \partial z^2} - u_0 \frac{\partial^3 w_1}{\partial z^3} \right. \\ & \quad - u_1 \frac{\partial^3 w_0}{\partial z^3} - \frac{\partial u_0}{\partial x} \frac{\partial^2 u_1}{\partial z^2} - \frac{\partial u_1}{\partial x} \frac{\partial^2 u_0}{\partial z^2} + w_0 \frac{\partial^3 u_1}{\partial z^3} \\ & \quad + w_1 \frac{\partial^3 u_0}{\partial z^3} - \frac{\partial u_0}{\partial z} \frac{\partial^2 w_1}{\partial z^2} - \frac{\partial u_1}{\partial z} \frac{\partial^2 w_0}{\partial z^2} \\ & \quad \left. + 2\frac{\partial w_0}{\partial z} \frac{\partial^2 u_1}{\partial z^2} + 2\frac{\partial w_1}{\partial z} \frac{\partial^2 u_0}{\partial z^2}\right), \tag{3.18} \end{aligned}$$

and

$$-\frac{\partial p_2}{\partial z} + \frac{\partial^2 w_0}{\partial z^2} + K\left[-2\frac{\partial u_0}{\partial z}\frac{\partial^2 u_1}{\partial z^2} - 2\frac{\partial u_1}{\partial z}\frac{\partial^2 u_0}{\partial z^2}\right] = 0. \tag{3.19}$$

The boundary conditions are

$$\text{at } z = 0, u_2 = 0, \quad w_2 = 0, \tag{3.20}$$

and, at $z = h(x, t)$,

$$-p_2 + 2\left(-h_x \frac{\partial u_0}{\partial z} + \frac{\partial w_0}{\partial z}\right) + K\left(-2 \frac{\partial u_0}{\partial z} \frac{\partial u_1}{\partial z}\right) = 0, \tag{3.21}$$

$$\begin{aligned} & \frac{\partial w_0}{\partial x} + \frac{\partial u_2}{\partial z} - h_x^2 \frac{\partial u_0}{\partial z} + 2h_x \left(\frac{\partial w_0}{\partial z} - \frac{\partial u_0}{\partial x}\right) + K \left[\frac{\partial^2 u_1}{\partial t \partial z} + u_0 \frac{\partial^2 u_1}{\partial x \partial z} \right. \\ & \quad + u_1 \frac{\partial^2 u_0}{\partial x \partial z} + w_0 \frac{\partial^2 u_1}{\partial z^2} + w_1 \frac{\partial^2 u_0}{\partial z^2} + \frac{\partial u_0}{\partial z} \frac{\partial w_1}{\partial z} + \frac{\partial u_1}{\partial z} \frac{\partial w_0}{\partial z} \\ & \quad \left. - \frac{\partial u_0}{\partial x} \frac{\partial u_1}{\partial z} - \frac{\partial u_1}{\partial x} \frac{\partial u_0}{\partial z} + 2h_x \left(-2 \frac{\partial u_0}{\partial z} \frac{\partial u_1}{\partial z}\right) \right] \\ & = 0. \end{aligned} \tag{3.22}$$

Using the results of the zeroth order (equation (3.7)) and first order (equations (3.14)–(3.16)), the solution of the second-order problem (equations (3.17)–(3.22)) satisfies

$$\begin{aligned} u_2 &= \left(\frac{z^4}{24} - \frac{h^3 z}{6}\right)g_1(x, t) + \left(\frac{z^3}{6} - \frac{h^2 z}{2}\right)g_2(x, t) + \left(\frac{z^2}{2} - hz\right)g_3(x, t) \\ & \quad + z[U_{xx}h + 4U_x h_x + Kf(h_t + Uh_x + U_x h)], \\ w_2 &= \left(-\frac{z^5}{120} + \frac{h^3 z^2}{12}\right)\frac{\partial g_1}{\partial x} + \frac{z^2 h^2 h_x}{4}g_1 + \left(-\frac{z^4}{24} + \frac{h^2 z^2}{4}\right)\frac{\partial g_2}{\partial x} \\ & \quad + \frac{z^2 h h_x}{2}g_2 + \left(-\frac{z^3}{6} + \frac{h z^2}{2}\right)\frac{\partial g_3}{\partial x} + \frac{z^2}{2}h_x g_3 \\ & \quad - \frac{z^2}{2}\frac{\partial}{\partial x}[U_{xx}h + 4U_x h_x + Kf(h_t + Uh_x + U_x h)], \quad \text{and} \\ p_2 &= -2U_x, \end{aligned}$$

where $g_1(x, t) = f_t + Uf_x - U_x f$, $g_2(x, t) = -(h_t + Uh_x)f - hf_t - Uh_x f$, and $g_3(x, t) = -3U_{xx} - K(f_t + Uf_x - 3U_x f)$.

3.4. Thin-film equation Using the kinematic boundary condition, the free-surface evolution equation can be obtained as

$$\frac{\partial h}{\partial t} + \frac{\partial}{\partial x} F(h) = 0, \tag{3.23}$$

where

$$\begin{aligned} F(h) &= Uh - \epsilon \frac{h^3 f}{3} + \epsilon^2 \left[\frac{-3h^5}{40}(f_t + Uf_x - U_x f) - \frac{5h^4}{24}(-h_t f - hf_t - Uh_x f - Uh_x f) \right. \\ & \quad - \frac{h^3}{3}(-3U_{xx} - Kf_t - KU_x f + 3KU_x f) \\ & \quad \left. + \frac{h^2}{2}(U_{xx}h + 4U_x h_x + Kfh_t + KfUh_x + KfU_x h) \right] \end{aligned}$$

and $f(x, t) = U_t + UU_x + Fr h_x - Sh_{xxx}$.

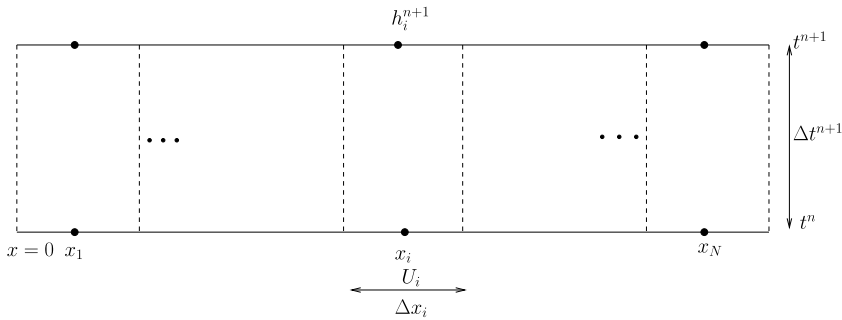


FIGURE 2. Typical grid used for finite-volume discretizations. The bold black dots and dashed vertical lines represent the nodal points and the cell faces, respectively. The symbol U_i stands for the stretching sheet velocity at the centre of the i th cell and Δx_i is the grid size of the cell $[x_{i-1/2}, x_{i+1/2}]$.

The closure of the thin-film equation requires the boundary condition for the film height. At the origin, we apply the symmetric boundary condition, that is, $h_x = 0$, $h_{xxx} = 0$, and $h_{xxxx} = 0$ and, at the other end of the domain, we assume that the same sheet stretching rate continues beyond the computed domain. We also assume that the gradient of the free surface extends out of the computational domain. These boundary conditions are consistent with those mentioned by Santra et al. [24]. Finally, the model equation is supported by the initial condition $h(x, 0) = 1 + \delta(x)$.

4. Numerical procedure

Many kinds of numerical methods such as a combination of the Euler method and the Newton–Kantorovich method were presented in the recent past [13, 24] for this kind of nonlinear convection–diffusion equation. In this paper, we follow the finite-volume method on a uniform grid system with implicit flux discretization as described by Panda et al. [21] and Sellier and Panda [25].

As shown in Figure 2, we discretized the fluid domain using a uniform grid. The variables like film thickness h and stretching velocity U are located at the cell centres. Let the flow domain $[0, L]$ be discretized into N equal size grid cells of size $\Delta x_i = L/N$ and define $x_i = \Delta x_i/2 + (i - 1)\Delta x_i$, $i = 1, 2, \dots, N$, so that x_i is the centre of the cell. Since the sizes of the grids are uniform, we denote Δx instead of Δx_i . The edges of the cell i are then located at $x_{i-1/2} = x_i - \Delta x_i/2$ and $x_{i+1/2} = x_i + \Delta x_i/2$. The numerical solution is evaluated at the discrete time levels t^n , $n = 0, 1, 2, \dots$ with time step $\Delta t^{n+1} = t^{n+1} - t^n$. The film thickness h is approximated over the cell $[x_{i-1/2}, x_{i+1/2}]$ in order to get the discretized equation. The approximation of the cell average of the solution over the grid cell is

$$h_i^n \sim h(x_i, t^n) = \frac{1}{\Delta x_i} \int_{x_{i-1/2}}^{x_{i+1/2}} h(x, t^n) dx.$$

From the given solution h_i^n , the solution at the next time step t^{n+1} is obtained by integrating equation (3.23) over the space and time intervals $[x_{i-1/2}, x_{i+1/2}] \times [t^n, t^{n+1}]$,

which gives the discretized equation

$$(h_i^{n+1} - h_i^n)\Delta x_i + (F_{i+1/2}^{n+1} - F_{i-1/2}^{n+1})\Delta t^{n+1} = 0 \tag{4.1}$$

for nodes $i = 1, 2, \dots, N$, where the discrete flux function $F_{i+1/2}^{n+1} = F(x_{i+1/2}, t^{n+1})$.

For the internal nodes, the face values are evaluated using linear interpolation from nodal values and the gradients at the cell faces are evaluated using central differences.

Similarly, the second-, third-, and fourth-order derivatives are discretized as

$$\begin{aligned} h_{xx}(x_{i+1/2}, t^{n+1}) &= \frac{1}{\Delta x^2}(h_{i+1}^{n+1} - 2h_i^{n+1} + h_{i-1}^{n+1}) + O(\Delta x), \\ h_{xxx}(x_{i+1/2}, t^{n+1}) &= \frac{1}{\Delta x^3}(h_{i+2}^{n+1} - 3h_{i+1}^{n+1} + 3h_i^{n+1} - h_{i-1}^{n+1}) + O(\Delta x^2), \\ h_{xxxx}(x_{i+1/2}, t^{n+1}) &= \frac{1}{\Delta x^4}(h_{i+3}^{n+1} - 4h_{i+2}^{n+1} + 6h_{i+1}^{n+1} - 4h_i^{n+1} + h_{i-1}^{n+1}) + O(\Delta x). \end{aligned}$$

The above derivative expressions are valid for the internal nodes $i = 3$ to $N - 3$, and we need different expressions for the higher order derivatives for the nodes present at the positions $i = 1, 2$ and $i = N - 2, N - 1$, and $i = N$. For the boundary node, for example, at $i = 1$, we have the following approximations of the derivatives:

$$\begin{aligned} h_{xxx}(x_{1+1/2}, t^{n+1}) &= \frac{1}{\Delta x^3}(h_3^{n+1} - 3h_2^{n+1} + 3h_1^{n+1} - h_0^{n+1}) + O(\Delta x^2), \\ h_{xxxx}(x_{1+1/2}, t^{n+1}) &= \frac{1}{\Delta x^4}(h_4^{n+1} - 4h_3^{n+1} + 6h_2^{n+1} - 4h_1^{n+1} + h_0^{n+1}) + O(\Delta x). \end{aligned}$$

In order to compute h_0 , we introduce the ghost cell $i = 0$, which is located just outside the domain. The boundary condition is used to fill these cells with values h_0 and based on the values h_i in the interior cells. Similarly, we approximate the higher order derivatives of h at the other boundary nodes incorporating the information on boundary conditions and using the interpolated value of h at the boundary.

The values of the function U and its derivative are known at the control volume centre. The time-derivative term which appears in flux due to the second-grade fluid properties is approximated with first-order forward difference.

Equation (4.1) describes an implicit time-discretization scheme. Since the governing equation is nonlinear, a system of nonlinear algebraic equations needs to be solved at each time step. We use `FSOLVE` in `MATLAB` for this purpose. We start the simulation with given initial film thickness $1 + \delta(x)$ with time step $\Delta t = 0.01$ and spatial resolution $\Delta x = 0.05$. Convergence is usually achieved in less than 20 iterations and the convergence criterion is that the norm of the residuals should be less than 10^{-7} .

5. Result analysis

5.1. Steady stretching surface To demonstrate the successful implementation of the proposed finite-volume scheme, the numerical results obtained with the proposed algorithm are first compared to those obtained by Santra et al. [24] for the steady

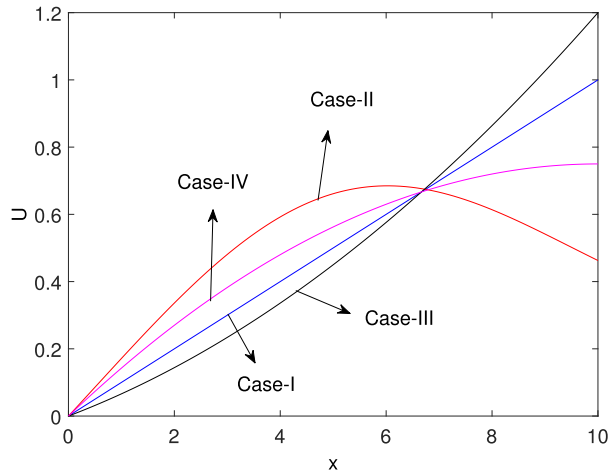


FIGURE 3. Various steady stretching velocities U against x .

stretching profile, that is, $U(x, t) = U(x)$. For this benchmark case, we consider here the four different types of stretching velocity profiles proposed by Santra et al. [24] to allow direct comparison in the Newtonian cases:

Case I (linear)	$U(x) = 0.1x,$
Case II (nonmonotonic)	$U(x) = 0.92542(-0.535261 + 0.05x + e^{-0.025(x-5)^2}),$
Case III (parabolic concave)	$U(x) = 0.6(0.1x + 0.01x^2),$
Case IV (parabolic convex)	$U(x) = 0.75[1 - (0.1x - 1)^2].$

(5.1)

The equations (5.1) are plotted in Figure 3. In the following the free surfaces are analysed for different stretching velocity profiles.

The effect of the stretching velocity distribution on film height at different times is shown in Figure 4 with $\epsilon = 0.1, S = 0.1, Fr = 0.1,$ and $K = 0$ with initial thickness $h(x, 0) = 1 + \delta(x) = 1 - x^2/130$. The parameters and the initial condition are chosen for the direct comparison with the work of Santra et al. [24].

The left upper panel (Figure 4) illustrates the free-surface profile for the linear stretching velocity given by equation (5.1) (Case I). The initial deformation of the free surface is advected downstream by the stretching velocity and, with the advancement of time, the profile becomes flatter. The upper right panel corresponds to the nonmonotonic stretching velocity profile (equation (5.1), Case II) which shows the increase of film height at large spatial value x . Because the stretching rate decreases for large x , as a result, the fluid that comes from upstream loses its momentum. The lower left panel illustrates the height of the thin film for a given parabolic concave profile. Note that the higher stretching velocity is responsible for making the thin film thinner at large x whereas the opposite effect can be observed in the lower right panel that shows the effect of a parabolic convex stretching profile on the free surface of the

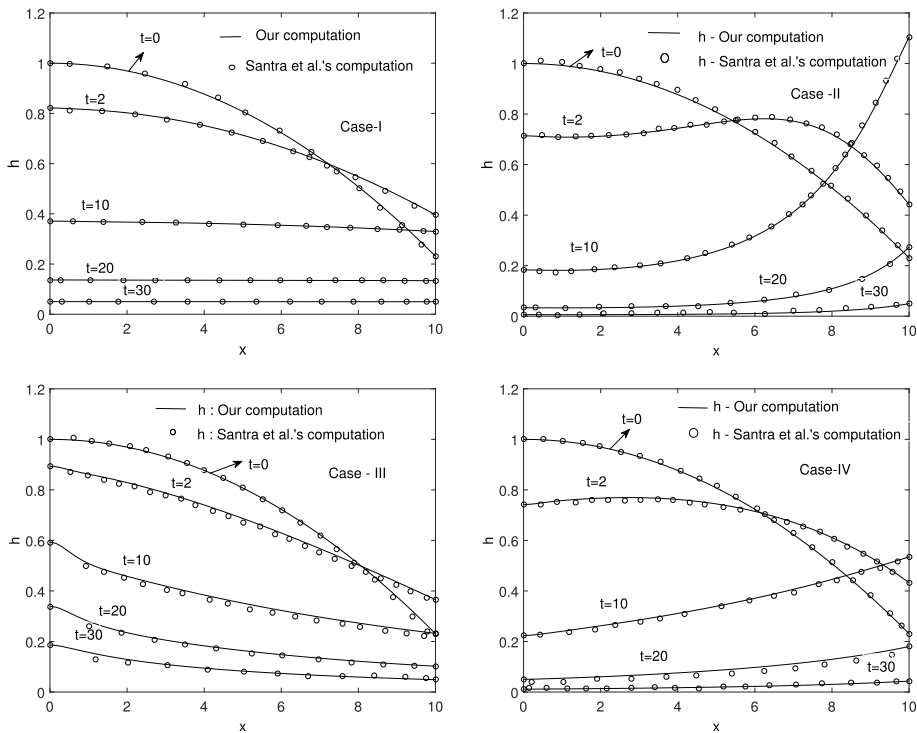


FIGURE 4. Free-surface profile at different times for different stretching velocity distributions as given by equations (5.1) with $S = 0.1$, $F = 0.1$, $\epsilon = 0.1$, and $h(x, 0) = 1 - x^2/130$.

flow. These results comply well with the discussion by Santra et al. [24] and validate the implementation of the finite-volume scheme.

The approach outlined above results in a free surface of the thin-film solution for the given mesh $\Delta x = 0.05$. Although it validates implementation and compares well with the available literature solution, we need to make sure that the solution is also independent of mesh and time resolution. In order to study the sensitivity of the solution to discretization parameters, we have plotted the film thickness profile against the distance of the stretching sheet for different grid sizes (left-hand panel of Figure 5).

The stretching profile, Case I with $\epsilon = 0.1$, $F = 0.1$, $S = 0.1$, and $\delta(x) = 1 - x^2/130$, was used for the simulation. It can be seen that within the grid size range $\Delta x \in \{0.15, 0.1, 0.05\}$ the solution is independent of the mesh resolution. The right-hand panel of Figure 5 also shows the results of calculation of different time steps. It can be observed that the computations are independent of the time steps. In the computation of the following results a grid size $\Delta x = 0.1$ and a time step $\Delta t = 0.05$ are chosen.

The success of the results for a small value of $\epsilon = 0.1$ in Figure 4 motivated us to check whether the second-order-term contribution will be small compared to the first-order term. We try the solution for a large value of $\epsilon = 0.3$ for two reasons: (i) to see

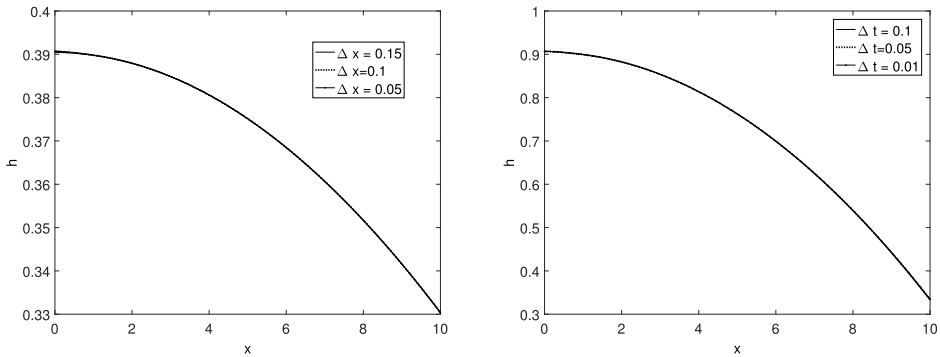


FIGURE 5. Mesh and time independent study: left: film thickness profile for different grid sizes with time step $\Delta t = 0.05$, right: film thickness profile for different time steps with grid size $\Delta x = 0.1$.

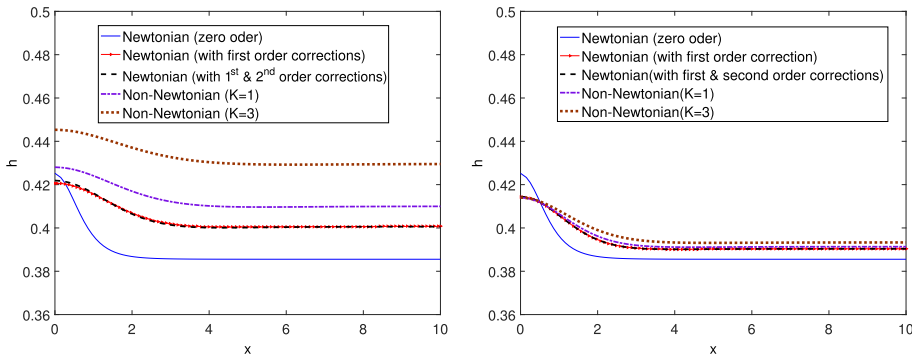


FIGURE 6. Solution of the free-surface profile at different orders of asymptotic solutions with $S = 1.0$, $Fr = 1.0$, $U = x$, $h(x, t = 0) = 1 + 0.1e^{-(x/0.25)^2/2}$ at fixed time $t = 1$, left: film thickness profile for $\epsilon = 0.3$, right: film thickness profile for $\epsilon = 0.1$.

any contribution of the second-order correction term to the first-order solution for the Newtonian case; (ii) the interest in the study is to explore the non-Newtonian effects on the free surface of the thin-film flow, which appears at the second order in the asymptotic expansion. The effect of the second-order term is shown in Figure 6.

The left-hand panel shows free-surface distributions for $\epsilon = 0.3$, and the right-hand panel is for $\epsilon = 0.1$. The linear stretching velocity profile $U = x$ is considered for this purpose, and the free-surface profiles for various values of K are plotted at a fixed time $t = 1$ (nondimensional). For the initial film thickness, a Gaussian profile is considered, that is,

$$h(x, t = 0) = 1 + \delta(x) = 1 + 0.1e^{-(x/0.25)^2/2} \tag{5.2}$$

to have small initial deformation. The value 0.25 in equation (5.2) represents the width of a Gaussian profile, and 0.1 is the depth of the hill in the initial thickness. The results confirm that the second-order correction term has a negligible effect on the

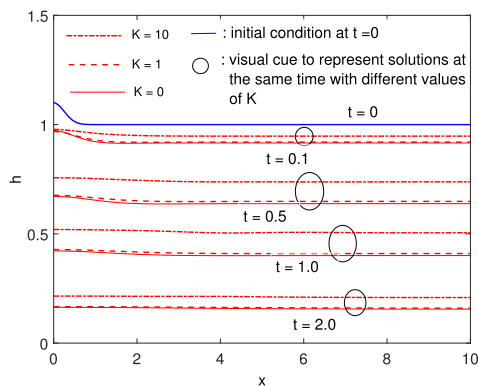


FIGURE 7. Variation of film height with x for different values of K with $S = 1.0$, $Fr = 1.0$, $\epsilon = 0.3$, $U = x$, and $h(x, t = 0) = 1 + 0.1e^{-(x/0.25)^2/2}$.

solution of the Newtonian ($K = 0$) thin-film equation. But, the effect of the second-grade Newtonian parameter is apparent for the nonzero values of K and $\epsilon = 0.3$. It can be observed that the film thins slowly for the larger value of K . This is due to the fact that the second-grade parameter exerted resistance to the flow.

To see more clearly the influence of the viscoelastic parameter K on the film height at the different times, the thin-film height is shown in Figure 7. It is clear from this figure that the presence of the second-grade non-Newtonian parameter delays the thinning of the film. This is consistent with the work of Hayat et al. [14], who have shown that the presence of viscoelasticity decreases the draining rate for Couette flow with a free boundary.

In Figure 8, the calculated thin-film height at the origin, that is, $h(x = 0, t)$, for the different values of the second-grade parameter K is plotted against time t (nondimensional). This figure clearly shows the type of behaviour observed in Figure 7. As the time increases the film height at the origin $h(x = 0, t)$ decreases, and stress build-up effects are seen due to the presence of the second-grade parameter.

We explore next the effect of the stretching velocity U and the effect of the second-grade non-Newtonian parameter K on the free-surface profile. Using a linear stretching velocity, that is, $U = \eta x$, where $\eta \in [0.1, 1]$, the effect of K on the free-surface profile is discussed. In order to do that, we need to define a clear measure

$$E(t) = \frac{1}{2} \int_D (h_{sg} - h_n)^2 dx, \quad (5.3)$$

where h_{sg} is the second-grade fluid solution, h_n is the corresponding Newtonian solution ($K = 0$), and D is the flow domain. The left-hand panel of Figure 9 shows the measure function E computed from equation (5.3) as a function of time t for $U = \eta x$, where $\eta = 0.1$. Clearly, the larger the values of K , the greater the difference (relative to the case $K = 0$), because of the additional stresses the fluid needs to overcome flow. For $U = \eta x$, where $\eta = 1.0$, the rapid stretching of the film will result in the rapid build-up

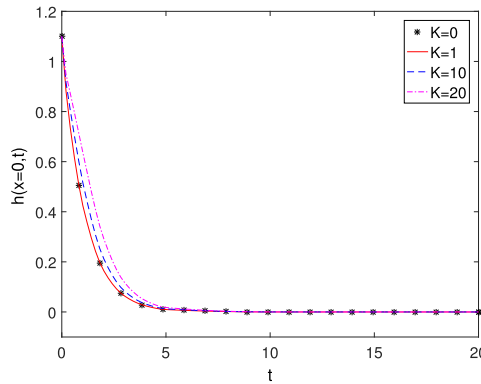


FIGURE 8. Effect of K on the variation of free surface at the origin for the stretching velocity $U = x$ with $S = 1.0$, $Fr = 1.0$, $\epsilon = 0.3$, and $h(x, t = 0) = 1 + 0.1e^{-(x/0.25)^2/2}$.

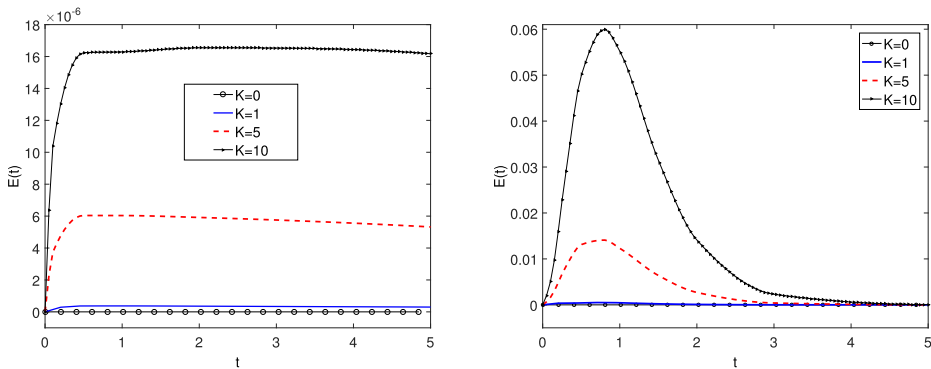


FIGURE 9. Error plot with $S = 1.0$, $Fr = 1.0$, $\epsilon = 0.3$, and initial profile equation (5.2), left: error plot for $U = \eta x$ ($\eta = 0.1$), right: error plot for $U = \eta x$ ($\eta = 1.0$).

of stresses. The faster the stretching, the higher the stress build-up. These stresses will relax over time and, finally, the difference E decreases (right-hand panel of Figure 9).

5.2. Unsteady stretching surface This section describes the dynamics of free-surface flow of a viscoelastic fluid over an unsteady stretching sheet. We consider that the surface velocity of the stretching sheet is unsteady [1]. The flow of the liquid film is caused by the stretching of the elastic surface at $z = 0$ and the sheet moves in the positive x -direction with the velocity

$$U(x, t) = \frac{bx}{1 - \alpha t}, \tag{5.4}$$

where b and α are positive constants. The effective stretching rate $b/(1 - \alpha t)$ increases with time, since $\alpha > 0$. It may be further noted that $1 - \alpha t > 0$, so the analysis is valid

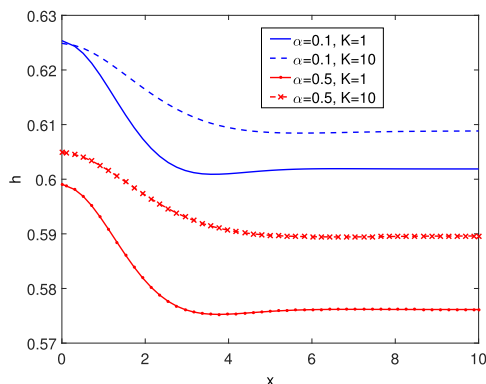


FIGURE 10. Effects of (K, α) on the free-surface profile with initial profile equation (5.2) and $S = 1.0$, $Fr = 1.0$, $\epsilon = 0.3$, $b = 1.0$, and at fixed time $t = 0.5$.

only for the time $t < 1/\alpha$. This means that, the smaller the value of α , the longer the time required to stretch the sheet.

With the given unsteady surface velocity equation (5.4), the free-surface profile of the viscoelastic fluid is given in Figure 10 for different values of α and the viscoelastic parameter K . For high values of K , the viscoelastic stresses relax more slowly, that is, they provide a resistance to the flow over a longer period of time: hence, the slower thinning rate observed for $K = 10$ compared to $K = 1$. The free surface becomes thinner with the smaller value of the viscoelastic parameter. The effect of K is much more prominent at the origin of the sheet when $\alpha = 0.5$, that is, for rapid stretching. This unsteady stretching results can be compared with the steady stretching sheet results given in Figure 7. The free-surface profile for unsteady stretching sheets exhibits similar fashions to those for the steady stretching sheet. It is also clear that the viscoelastic effect is similar for both the cases.

The velocity u as a function of z at different time levels with variations of α and K with $b = 1.0$, $S = 1.0$, $F = 1.0$, and $\epsilon = 0.3$ is plotted for $x = 2$ and $x = 7$ in Figure 11 (upper panel) and Figure 12 (upper panel), respectively. The corresponding thin-film profiles are given in Figure 13. The velocity profile at the fixed small value of $\alpha = 0.1$, for which the time required to stretch the sheet is more, is given in the left upper panel of Figure 11. It is clear from the figure (upper panel) that the velocity is maximum at the sheet and then decreases, and attains a minimum value at the top for the second-grade parameter $K = 1$. A similar pattern is observed for $\alpha = 0.5$ (right upper panel of Figure 11), where the time required to stretch the sheet is less. We observe that the velocity is higher for the higher values of K and the stress is also higher (lower panel of Figure 11).

The fluid velocity far away from the origin, that is, at $x = 7$, is higher in contrast to the results for the velocity at $x = 2$. In all cases, the value of the shear stress profile is higher close to the sheet and then approaches zero near the free surface due to the imposed boundary condition.

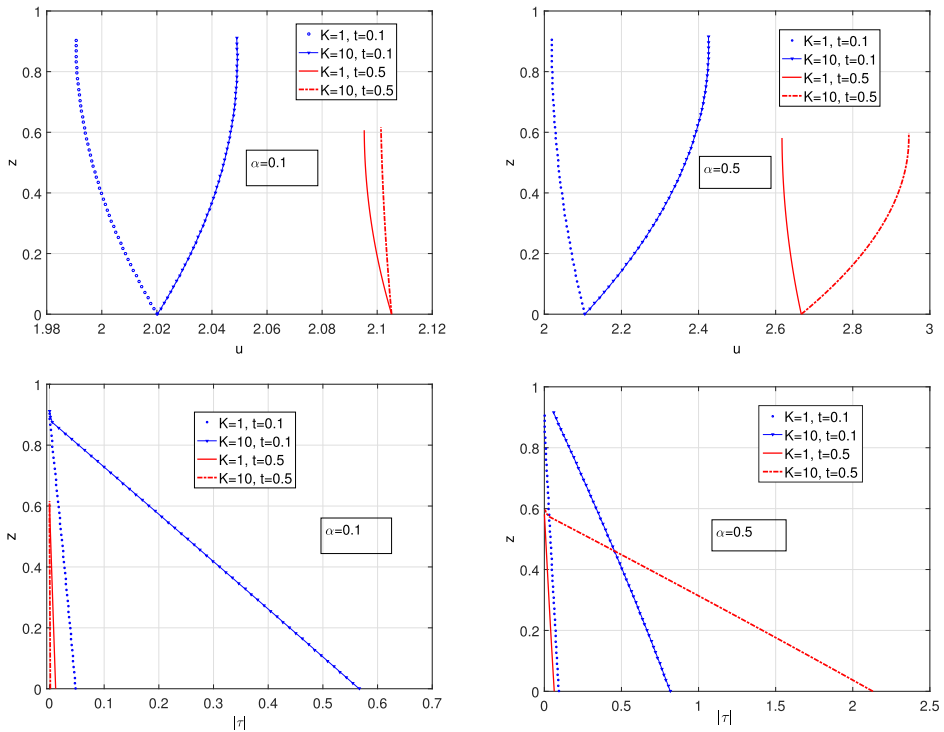


FIGURE 11. Effect of (α, K, t) on the velocity profile and shear stress against z at fixed $x = 2$ with $S = 1.0$, $F = 1.0$, $\epsilon = 0.3$, and $b = 1.0$, upper left: velocity profile at $\alpha = 0.1$, upper right: velocity profile at $\alpha = 0.5$, lower left: stress profile at $\alpha = 0.1$, lower right: stress profile at $\alpha = 0.5$.

6. Conclusion

In this work, we presented the long-wave theory for the derivation of a thin-film equation of a second-grade fluid over steady and unsteady stretching sheets. The model is an extension to the existing approaches, which only dealt with Newtonian fluids. Note that the Newtonian case is recovered by setting the second-grade parameter K to zero. We have developed a finite-volume code which is able to solve the highly nonlinear governing equations. The correct implementation of the numerical method is verified in the Newtonian case by comparing our results to those obtained by Santra et al. [24]. We observe that the presence of the second-grade parameter delays the thinning of the film over the steady as well as the unsteady stretching sheet. The numerical scheme was successfully tested for time-step and mesh convergence. The developed model shows that the viscoelastic effect only becomes prominent as a second-order correction. This is an important conclusion, which gives an indication of when such effect may be relevant to consider or not. We have also shown that the effect of viscoelasticity is to delay the thinning rate in accordance with an earlier work

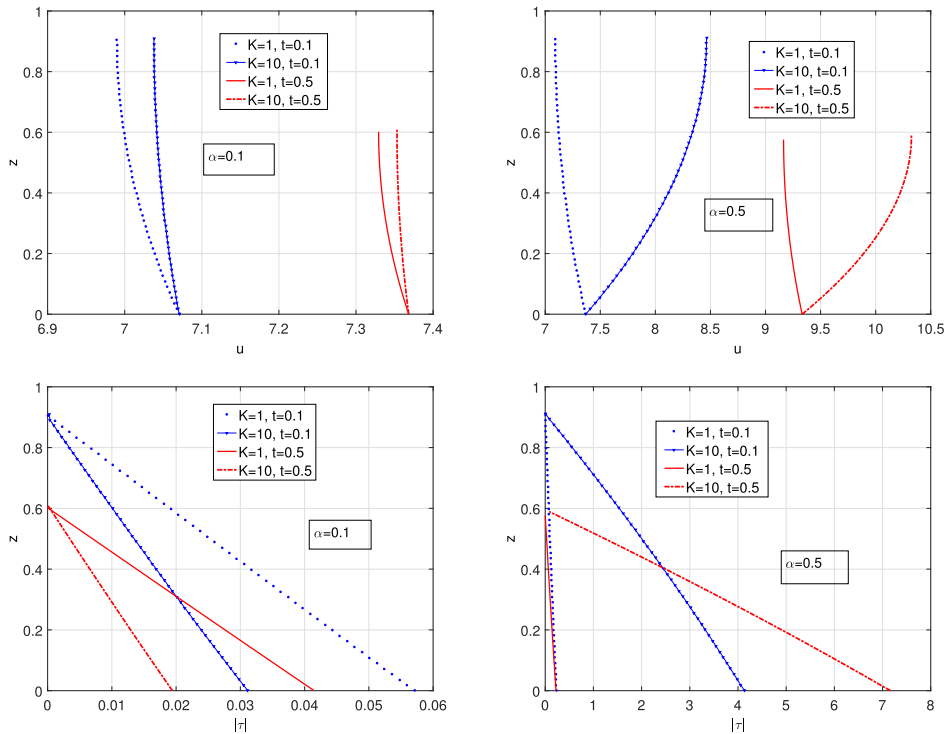


FIGURE 12. Same as mentioned in the caption of Figure 11 but at $x = 7$.

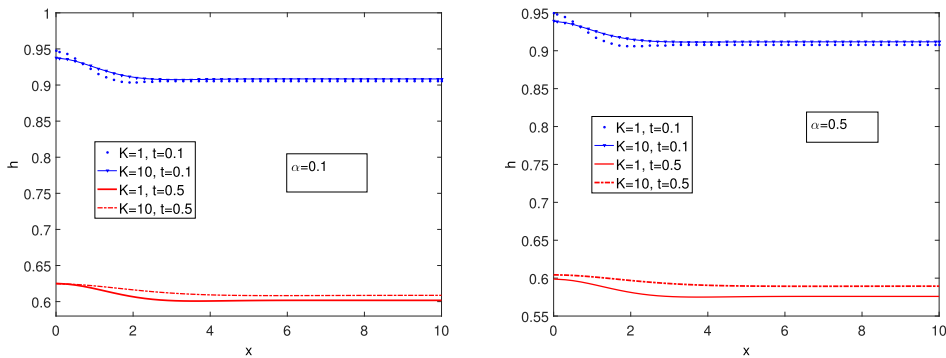


FIGURE 13. Corresponding free-surface profile, left: for $\alpha = 0.1$, right: for $\alpha = 0.5$.

of Hayat et al. [14], who only considered the fixed boundary case. This may have important physiological implications for the flow of the thin mucus layer which lines biological tissues.

References

- [1] Z. Abbas, T. Hayat, M. Sajid and S. Asghar, “Unsteady flow of a second grade fluid film over an unsteady stretching sheet”, *Math. Comput. Modelling* **48** (2008) 518–526; doi:j.mcm.2007.09.015.
- [2] I. Ahmad, “On unsteady boundary layer flow of a second grade fluid over a stretching sheet”, *Adv. Theor. Appl. Mech.* **6** (2013) 95–105; doi:atam.2013.231.
- [3] H. I. Andersson, J. B. Aarseth and B. S. Dandapat, “Heat transfer in a liquid film on an unsteady stretching surface”, *Int. J. Heat Mass Transfer* **43** (2000) 69–74; doi:S0017-9310(99)00123-4.
- [4] H. I. Andersson, K. H. Bech and B. S. Dandapat, “Magnetohydrodynamic flow of a power-law fluid over a stretching sheet”, *Int. J. Non-Linear Mech.* **27** (1992) 929–936; doi:0020-7462(92)90045-9.
- [5] L. J. Crane, “Flow past a stretching plate”, *Z. Angew. Math. Phys. ZAMP* **21** (1970) 645–647; doi:BF01587695.
- [6] B. S. Dandapat, A. Kitamura and B. Santra, “Transient film profile of thin liquid film flow on a stretching surface”, *Z. Angew. Math. Phys. ZAMP* **57**(2006) 623–635; doi:s00033-005-0040-7.
- [7] B. S. Dandapat and S. Maity, “Flow of a thin liquid film on an unsteady stretching sheet”, *Phys. Fluids* **18** (2006) 102101; doi:1.2360256.
- [8] B. S. Dandapat, S. Maity and A. Kitamura, “Liquid film flow due to an unsteady stretching sheet”, *Int. J. Non-Linear Mech.* **43** (2008) 800–886; doi:j.ijnonlinmec.2008.06.003.
- [9] B. S. Dandapat and S. K. Singh, “Thin film flow over a heated nonlinear stretching sheet in presence of uniform transverse magnetic field”, *Int. Commun. Heat Mass Transfer* **38** (2011) 324–328; doi:j.icheatmasstransfer.2010.11.009.
- [10] J. E. Dunn and R. L. Fosdick, “Thermodynamics, stability and boundedness of fluids of complexity 2 and fluids of second grade”, *Arch. Ration. Mech. Anal.* **56** (1974) 191–252; doi:BF00280970.
- [11] J. E. Dunn and K. R. Rajagopal, “Fluids of differential type: critical review and thermodynamics analysis”, *Internat. J. Engrg. Sci.* **33** (1995) 689–747; doi:0020-7225(94)00078-X.
- [12] R. L. Fosdick and K. R. Rajagopal, “Anomalous features in the model of second order fluids”, *Arch. Ration. Mech. Anal.* **70** (1979) 145–152; doi:BF00250351.
- [13] Y. Ha, Y. J. Kim and T. G. Myers, “On the numerical solution of a driven thin film equation”, *J. Comput. Phys.* **227** (2008) 7246–7263; doi:j.jcp.2008.04.007.
- [14] T. Hayat, M. Khan, A. M. Siddiqui and S. Asghar, “Transient flows of a second grade fluid”, *Int. J. Non-Linear Mech.* **39** (2004) 1621–1633; doi:j.ijnonlinmec.2002.12.001.
- [15] S. Kalliadasis, C. Ruyer-Quil, B. Scheid and M. G. Velarde, *Falling liquid films, Volume 176 of Appl. Math. Sci.* (Springer, London, 2012); doi:978-1-84882-367-9.
- [16] R. Levy, D. B. Hill, M. G. Forest and J. B. Grotberg, “Pulmonary fluid flow challenges for experimental and mathematical modeling”, *Integr. Comp. Biol.* **54** (2014) 985–1000; doi:icb/icu107.
- [17] I. C. Liu and H. I. Andersson, “Heat transfer in a liquid film on an unsteady stretching sheet”, *Int. J. Thermal Sci.* **47** (2008) 766–772; doi:j.ijthermalsci.2007.06.001.
- [18] S. Nadeem and N. Faraz, “Thin film flow of a second grade fluid over a stretching/shrinking sheet with variable temperature-dependent viscosity”, *Chin. Phys. Lett.* **27** (2010) 034704; doi:0256-307X/27/3/034704.
- [19] N. F. M. Noor, O. Abdulaziz and I. Hashim, “MHD flow and heat transfer in a thin liquid film on an unsteady stretching sheet by the homotopy analysis method”, *Internat. J. Numer. Methods Fluids* **63** (2010) 357–373; doi:fld.2078.
- [20] S. B. G. O’Brien and L. W. Schwartz, “Theory and modeling of thin film flows”, in: *Encyclopedia of surface and colloid science*, (Marcel Dekker, NY, USA, 2002) 5283–5297; <https://pdfs.semanticscholar.org/1cc5/1908e0dd5fbf43a8b8ed481844a1fc28f8e3.pdf>.
- [21] S. Panda, M. Sellier, M. C. S. Fernando and M. K. Abeyratne, “Process parameter identification in thin film flows driven by a stretching surface”, *Int. J. Engng Math.* **2014** (2014) 485431; doi:2014/485431.

- [22] K. R. Rajagopal and A. R. Srinivasa, “On the development of fluid models of the differential type within a thermodynamic framework”, *Mech. Res. Commun.* **35** (2008) 483–489; doi:j.mechrescom.2008.02.004.
- [23] R. S. Rivlin and J. L. Ericksen, “Stress deformation relations for isotropic materials”, *J. Ration. Mech. Anal.* **4** (1995) 323–425; doi:10.1007/978-1-4612-2416-7_61.
- [24] B. Santra and B. S. Dandapat, “Thin-film flow over a nonlinear stretching sheet”, *Z. Angew. Math. Phys. ZAMP* **60** (2009) 688–700; doi:s00033-008-8015-0.
- [25] M. Sellier and S. Panda, “Surface temperature reconstruction based on the thermocapillary effect”, *ANZIAM J.* **52** (2010) 146–159; doi:S1446181111000654.
- [26] C. Y. Wang, “Liquid film on an unsteady stretching sheet”, *Quart. Appl. Math.* **48** (1990) 601–610; doi:qam/1079908.